ACS OMEGA

Open Access

http://pubs.acs.org/journal/acsodf

Article

Unconventional Radical and Radical-Hole Site-Based Interactions in Halogen-Bearing Dimers and Trimers: A Comparative Study

Mahmoud A. A. Ibrahim,* Heba S. M. Abd Elhafez, Mohammed N. I. Shehata, Nayra A. M. Moussa, Shaban R. M. Sayed, Mahmoud E. S. Soliman, Muhammad Naeem Ahmed, Mohamed Khaled Abd El-Rahman, and Tamer Shoeib*

Cite This: *ACS Omega* 2024, 9, 38743−38752

Read Online

ACCESS | Metrics & More | Article Recommendations | Supporting Information

ABSTRACT: Radical ($R^{\bullet}$) and $R^{\bullet}$-hole site-based interactions are comparatively studied, for the first time, using *ab initio* methods. In this regard, $R^{\bullet}$-bearing molecules $^{\bullet}XO_3$ (where X = Cl, Br, and I) were subjected to direct interaction with NH_3 within dimeric and trimeric forms in the form of $NH_3\cdots{}^{\bullet}XO_3/{}^{\bullet}XO_3\cdots NH_3$ and $NH_3\cdots{}^{\bullet}XO_3\cdots NH_3$ complexes, respectively. As confirmed by electrostatic potential analysis, the studied $R^{\bullet}$-bearing molecules $^{\bullet}XO_3$ had the outstanding potentiality to interact as Lewis acid centers via two positive sites dubbed as $R^{\bullet}$ and $R^{\bullet}$-hole sites. Such an observation proposed the potentiality of the considered $^{\bullet}XO_3$ molecules to engage in unconventional $R^{\bullet}$ and well-established $R^{\bullet}$-hole site-based interactions with Lewis bases. This was confirmed by negative interaction (E_{int}) energies, ranging from −4.93 to −19.89 kcal/mol, with higher favorability for $R^{\bullet}$ site-based interactions over the $R^{\bullet}$-hole site-based ones. MP2 energetic features furnished higher preferability for the $R^{\bullet}$ site-based interactions than the $R^{\bullet}$-hole site-based ones in the case of chlorine- and bromine-bearing complexes, and the reverse was true for the iodine-bearing complexes. Moreover, elevated E_{int} values were recorded for the $NH_3\cdots{}^{\bullet}XO_3\cdots NH_3$ trimers over the $NH_3\cdots{}^{\bullet}XO_3$ and $^{\bullet}XO_3\cdots NH_3$ dimers, outlining the higher preference of the $^{\bullet}XO_3$ molecules to engage in $R^{\bullet}$ and $R^{\bullet}$-hole site-based interactions in the trimeric form over the dimeric one. These results might be considered a requisite linchpin for numerous forthcoming supramolecular chemistry and crystal engineering studies.

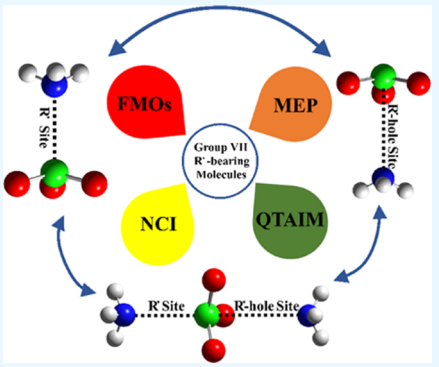

INTRODUCTION

Since the announcement of the crucial role of noncovalent interactions in sundry fields, including catalysis,[1,2] biological systems,[3−6] supramolecular chemistry,[7−9] and molecular recognition,[10−13] research societies began to strictly study the origin and nature of such crucial interactions. Astonishingly, σ-hole interactions are considered one of the most predominant noncovalent interactions as an upshot to their prevalent contributions in perceiving many vital applications.[2,14−21] The σ-hole concept was first reported to describe an electron-deficient region that appeared along the extension of the σ-bond of the covalently bonded group IV−VII elements.[15,16,22−26] Over the surface of the above-mentioned atoms, π- and lone pair (lp)-holes were afterward addressed[27−30] by the presence of depletion in the electron density that is located nearly perpendicular to the framework of the molecular entity[27,31] and in opposite to the lp,[32−34] respectively.

In addition to the above-mentioned hole concept, in-depth systematic studies were recently conducted, with more efforts being directed toward clarifying the characteristics of radical ($R^{\bullet}$)-hole sites and their corresponding interactions. The term $R^{\bullet}$-hole is defined as an area with a deficiency of electron density that is nearly opposite to the single electron of the $R^{\bullet}$-bearing molecules.[35] As a starting point, studying the $R^{\bullet}$-hole interactions of the $^{\bullet}TF_3$ molecules (T = tetrel atom) with Lewis bases showed apparent preferability in coincidence with the atomic size of the radical centers (i.e., C < Si < Ge).[35] Afterward, the strength of $R^{\bullet}$-hole interactions exhibited by group IV−VII $R^{\bullet}$-bearing molecules was disclosed, and it was found to increase as follows: $^{\bullet}SiF_3\cdots$ < $^{\bullet}POF_2\cdots$ < $^{\bullet}SO_2F\cdots$ < $^{\bullet}ClO_3\cdots$Lewis base complexes.[36]

According to the literature, the $R^{\bullet}$-bearing molecules revealed a prevalent potentiality to interact with Lewis acids via the unpaired electron (i.e., $R^{\bullet}$ site), forming single-electron noncovalent interactions.[37−41] In addition, various studies evinced the proton−acceptor behavior of $R^{\bullet}$-bearing molecules in hydrogen-bonded complexes of $HF\cdots{}^{\bullet}CH_3$,[42−44] $NH_3\cdots{}^{\bullet}CH_3$,[45] $OH_2\cdots{}^{\bullet}CH_3$,[46−48] $NCH\cdots{}^{\bullet}CH_3$,[49−51] and $HCCH\cdots{}^{\bullet}CH_3$.[52] Consequently, $R^{\bullet}$-bearing molecules may

Received: May 15, 2024
Revised: June 21, 2024
Accepted: July 31, 2024
Published: September 5, 2024

exhibit an amphoteric nature, nucleophilic character through their R•-hole site and electrophilic character through their single-electron R• site. However, the nucleophilic character of R•-bearing molecules through the R•-site has not been systematically studied yet.

In this regard, the present work was devoted to examining the ability of sp^2-hybridized group VII R•-bearing molecules to favorably engage in R• site-based interactions within the $NH_3\cdots{}^{\bullet}XO_3$ dimers (where X = Cl, Br, and I). In a parallel manner, the R•-hole site-based interactions were comparatively investigated in the ${}^{\bullet}XO_3\cdots NH_3$ dimers. For the first time, the potentiality of the investigated molecules to synchronously engage in R• and R•-hole site-based interactions was explored employing the $NH_3\cdots{}^{\bullet}XO_3\cdots NH_3$ trimers (Figure 1). The

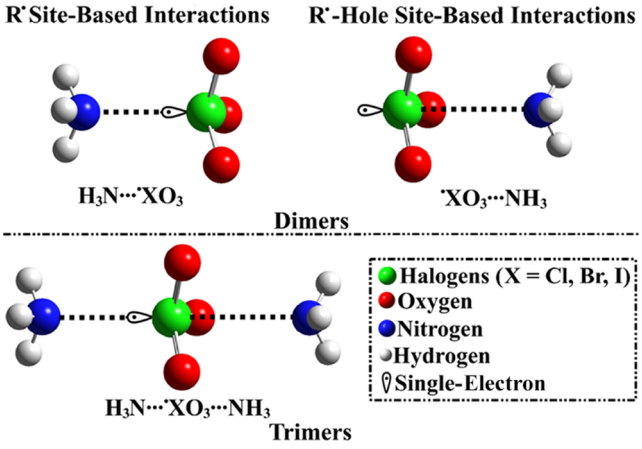

Figure 1. Illustrative representation of the R• and R•-hole site-based interactions within dimeric and trimeric forms in the form of $NH_3\cdots{}^{\bullet}XO_3/{}^{\bullet}XO_3\cdots NH_3$ and $NH_3\cdots{}^{\bullet}XO_3\cdots NH_3$ complexes, respectively.

obtained findings will provide a basis for forthcoming works relevant to the interactions of R•-bearing molecules with Lewis bases that would accordingly level up their admissible applications in supramolecular chemistry.

COMPUTATIONAL METHODS

The current study was established to comparatively explore the potential of the sp^2-hybridized group VII R•-bearing molecules (${}^{\bullet}XO_3$) to engage in R• and R•-hole site-based interactions via the $NH_3\cdots{}^{\bullet}XO_3$ and ${}^{\bullet}XO_3\cdots NH_3$ dimers, respectively. The trimeric form of the studied interactions was then considered in the form of $NH_3\cdots{}^{\bullet}XO_3\cdots NH_3$ complexes to investigate the simultaneous potentiality of the examined systems to participate in R• and R•-hole site-based interactions.

All of the calculations were performed using Gaussian09 software[53] by the MP2 method[54] with the aug-cc-pVTZ basis set for H,[55] N,[55] O,[55] and Cl[56] atoms. The aug-cc-pVTZ(PP) basis set was devoted to the case of Br[57] and I[57,58] atoms. The adopted nonstandard basis sets were obtained from the EMSL Basis Set Exchange Library.[59−61] First, geometry optimization calculations were carried out for the explored monomers, dimers, and trimers.

Upon optimization of ${}^{\bullet}ClO_3$, ${}^{\bullet}BrO_3$, and ${}^{\bullet}IO_3$ systems, EP analysis was performed using a 0.002 au electron density, as recommended earlier, by dint of its worthy depiction for the surface of chemical molecules.[62] Molecular electrostatic potential (MEP) maps were accordingly generated to envision the relative nucleophilicity and electrophilicity. Also, the surface electrostatic potential extrema (i.e., $V_{s,min}/V_{s,max}$) were quantified with the incorporation of Multiwfn 3.7 software.[63]

Upon optimization of $NH_3\cdots{}^{\bullet}XO_3/{}^{\bullet}XO_3\cdots NH_3$ dimers and $NH_3\cdots{}^{\bullet}XO_3\cdots NH_3$ trimers, the interaction energy (E_{int}) was assessed as the variation in energy between the complex and the sum of its monomers in the complex form. Moreover, the basis set superposition error (BSSE) was eradicated from the computed interaction energies using the counterpoise correction procedure.[64] The optimized complexes were not subjected to frequency calculations; therefore, it is feasible that these structures do not correspond to the true minima. For all investigated complexes, spin contamination was measured by the expectation value of the S^2 operator. The S^2 values were in the range of 0.7516−0.7589 after annihilation, confirming that spin contamination is negligible.

Benchmarking the MP2 interaction energies was done toward bestowing a more quantitative precision at the CCSD(T)/CBS level of theory based on eqs 1−3.[65,66]

$$E_{CCSD(T)/CBS} = \Delta E_{MP2/CBS} + \Delta E_{CCSD(T)} \quad (1)$$

where

$$\Delta E_{MP2/CBS} = (64E_{MP2/aug\text{-}cc\text{-}pVQZ} - 27E_{MP2/aug\text{-}cc\text{-}pVTZ})/37 \quad (2)$$

$$\Delta E_{CCSD(T)} = E_{CCSD(T)/aug\text{-}cc\text{-}pVDZ} - E_{MP2/aug\text{-}cc\text{-}pVDZ} \quad (3)$$

Quantum theory of atoms in molecules (QTAIM)[67] was accomplished to adequately elucidate the origin of the investigated interactions. Using QTAIM, we built the bond paths (BPs) and the bond critical points (BCPs) to indicate the origin of the investigated dimers and trimers. For a precise investigation of the origin of the considered interactions, various topological parameters, including the total energy density (H_b), electron density (ρ_b), and Laplacian ($\nabla^2\rho_b$) were extracted. In addition to QTAIM, noncovalent interaction (NCI)[6] index computations were conducted to precisely pinpoint and visualize the nature of noncovalent interactions exhibited by the R• and R•-hole sites. QTAIM and NCI index analyses were performed to generate the WFN files upon optimization of the complexes at the same level of theory with the help of Gaussian09 software. Based on the extracted WFN files, the QTAIM and NCI plots were built with the aid of the Multiwfn 3.7 software package[63] and were plotted via Visual Molecular Dynamics software.[68]

Using frontier molecular orbital (FMO) theory, the electronic parameters were evaluated for the investigated systems after and before the complexation process. Pictorially, the highest occupied molecular orbital (HOMO) and the lowest unoccupied molecular orbital (LUMO) distributions were pictured for the monomers and complexes under study. Additionally, the energy of HOMO (E_{HOMO}), energy of LUMO (E_{LUMO}), Fermi-level energy (E_{FL}), and the energy gap (E_{gap}) were numerically assessed through eqs 4 and 5:

$$E_{FL} = E_{HOMO} + \frac{E_{LUMO} - E_{HOMO}}{2} \quad (4)$$

$$E_{gap} = E_{LUMO} - E_{HOMO} \quad (5)$$

Moreover, the electronic properties, including global softness (S), chemical potential (μ), ionization potential (IP), electron affinity (EA), global hardness (η), work function (Φ), and

https://doi.org/10.1021/acsomega.4c04620
ACS Omega 2024, 9, 38743−38752

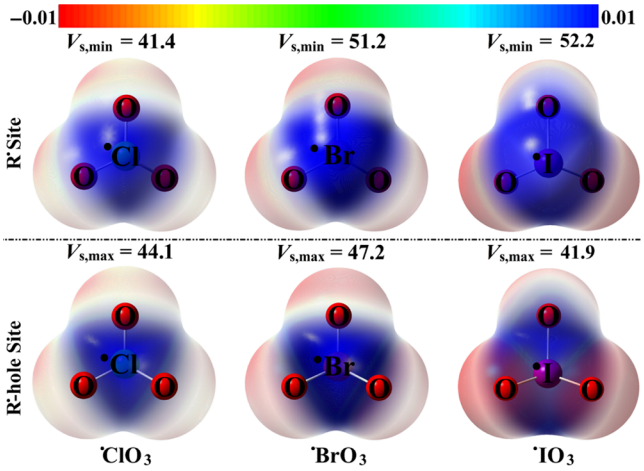

Figure 2. MEP maps of the R$^{\bullet}$ and R$^{\bullet}$-hole sites over the optimized $^{\bullet}XO_3$ molecules. The values of $V_{s,min}/V_{s,max}$ are given in kcal/mol.

electrophilicity index (ω) were assessed for the optimized monomers and complexes using eqs 6−12. It is worth mentioning that the vacuum-level electrostatic potential ($V_{eL}(+\infty)$) was set to nearly 0 within the work function estimation.

$$\mathrm{IP} \simeq -E_{HOMO} \tag{6}$$

$$\mathrm{EA} \simeq -E_{LUMO} \tag{7}$$

$$\eta = \frac{E_{LUMO} - E_{HOMO}}{2} \tag{8}$$

$$\mu = \frac{E_{LUMO} + E_{HOMO}}{2} \tag{9}$$

$$s = \frac{1}{\eta} \tag{10}$$

$$\omega = \frac{\mu^2}{2\eta} \tag{11}$$

$$\Phi = V_{eL(+\infty)} - E_{FL} \tag{12}$$

RESULTS AND DISCUSSION

EP Calculations. EP analysis was devoted to inspecting the nucleophilic and electrophilic sites over the molecular entities according to previous recommendations.[26,69] For the EP analysis, the MEP maps were generated for the $^{\bullet}XO_3$ molecules using a 0.002 au electron density envelope. Moreover, $V_{s,min}/V_{s,max}$ calculations were performed to numerically compute the magnitude of the positive R$^{\bullet}$ and R$^{\bullet}$-hole sites. Figure 2 displays the MEP maps and $V_{s,min}/V_{s,max}$ values.

Table 1. E_{int} and $E_{CCSD(T)/CBS}$ of the Dimeric and Trimeric Forms of R$^{\bullet}$ and R$^{\bullet}$-Hole Site-Based Interactions in the Form of $NH_3\cdots{}^{\bullet}XO_3/{}^{\bullet}XO_3\cdots NH_3$ and $NH_3\cdots{}^{\bullet}XO_3\cdots NH_3$ Complexes, Respectively, in kcal/mol and X···N Intermolecular Distances (d_1 and d_2) in Å

		distance			
	complex	d_1	d_2	E_{int}	$E_{CCSD(T)/CBS}$
dimers	R$^{\bullet}$ Site-Based Interactions				
	$H_3N\cdots{}^{\bullet}ClO_3$	2.80		−6.01	−5.90
	$H_3N\cdots{}^{\bullet}BrO_3$	2.83		−7.59	−7.29
	$H_3N\cdots{}^{\bullet}IO_3$	2.91		−9.05	−8.55
	R$^{\bullet}$-Hole Site-Based Interactions				
	$^{\bullet}ClO_3\cdots NH_3$		2.90	−4.93	−5.05
	$^{\bullet}BrO_3\cdots NH_3$		2.84	−6.44	−6.86
	$^{\bullet}IO_3\cdots NH_3$		2.47	−14.82	−16.10
trimers	R$^{\bullet}$ and R$^{\bullet}$-Hole Site-Based Interactions				
	$H_3N\cdots{}^{\bullet}ClO_3\cdots NH_3$	2.93	2.99	−9.52	−9.55
	$H_3N\cdots{}^{\bullet}BrO_3\cdots NH_3$	2.98	2.94	−12.02	−12.32
	$H_3N\cdots{}^{\bullet}IO_3\cdots NH_3$	3.01	2.51	−19.89	−21.19

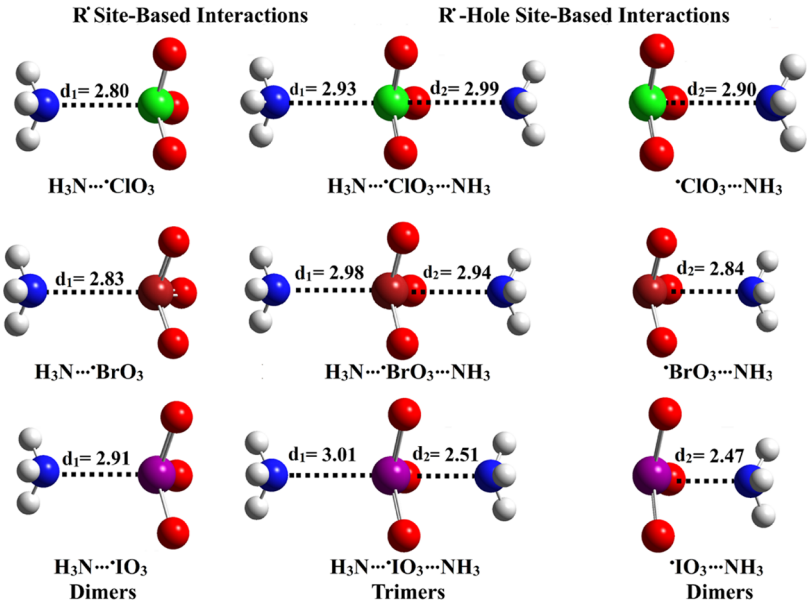

Figure 3. Optimized structures of the dimeric and trimeric forms of R$^{\bullet}$ and R$^{\bullet}$-hole site-based interactions in the form of $NH_3\cdots{}^{\bullet}XO_3/{}^{\bullet}XO_3\cdots NH_3$ and $NH_3\cdots{}^{\bullet}XO_3\cdots NH_3$ complexes, respectively. The X···N optimum distances are evaluated in Å.

https://doi.org/10.1021/acsomega.4c04620
ACS Omega 2024, 9, 38743−38752

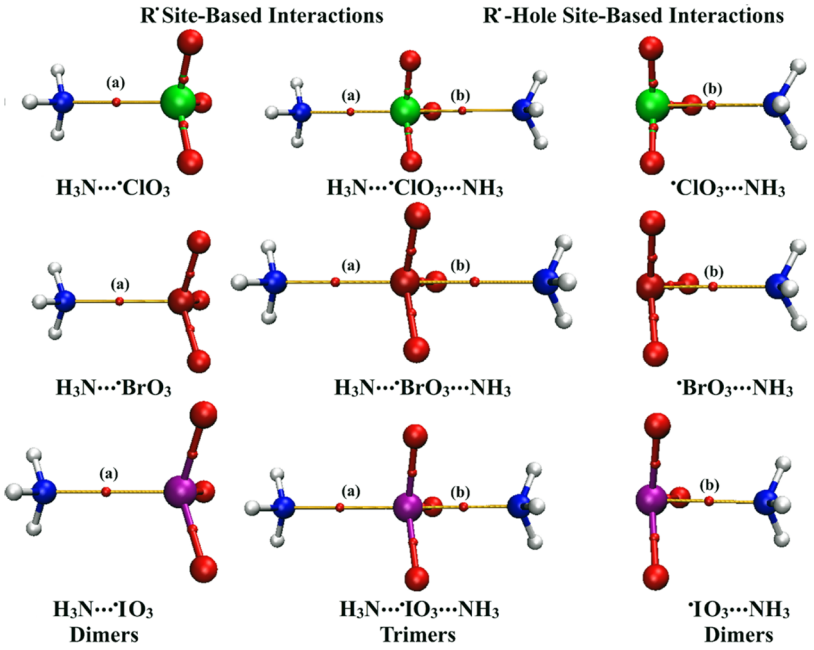

Figure 4. QTAIM diagrams of dimeric and trimeric forms of R$^{\bullet}$ and R$^{\bullet}$-hole site-based interactions in the form of $NH_3\cdots{}^{\bullet}XO_3/{}^{\bullet}XO_3\cdots NH_3$ and $NH_3\cdots{}^{\bullet}XO_3\cdots NH_3$ complexes, respectively. BCP locations are indicated by red dots. The symbols (a) and (b) refer to the generated BCPs within the R$^{\bullet}$ and R$^{\bullet}$-hole site-based interactions, respectively.

Table 2. Topological Parameters, Including $\nabla^2\rho_b$, ρ_b, and H_b at the Extracted BCPs within the Dimeric and Trimeric Forms of R$^{\bullet}$ and R$^{\bullet}$-Hole Site-Based Interactions in the Form of $NH_3\cdots{}^{\bullet}XO_3/{}^{\bullet}XO_3\cdots NH_3$ and $NH_3\cdots{}^{\bullet}XO_3\cdots NH_3$ Complexes, Respectively[a]

complex		ρ (au)	$\nabla^2\rho_b$ (au)	H_b (au)
dimers	R$^{\bullet}$ Site-Based Interactions			
	$H_3N\cdots{}^{\bullet}ClO_3$	0.0236	0.0676	0.0006
	$H_3N\cdots{}^{\bullet}BrO_3$	0.0255	0.0657	0.0001
	$H_3N\cdots{}^{\bullet}IO_3$	0.0276	0.0589	−0.0009
	R$^{\bullet}$-Hole Site-Based Interactions			
	$^{\bullet}ClO_3\cdots NH_3$	0.0162	0.0592	0.0013
	$^{\bullet}BrO_3\cdots NH_3$	0.0217	0.0656	0.0006
	$^{\bullet}IO_3\cdots NH_3$	0.0573	0.0700	−0.0153
trimers	R$^{\bullet}$ and R$^{\bullet}$-Hole Site-Based Interactions			
	$H_3N\cdots{}^{\bullet}ClO_3\cdots NH_3$	0.0177[b]/0.0134[c]	0.0536[b]/0.0505[c]	0.0012[b]/0.0014[c]
	$H_3N\cdots{}^{\bullet}BrO_3\cdots NH_3$	0.0190[b]/0.0176[c]	0.0517[b]/0.0561[c]	0.0008[b]/0.0010[c]
	$H_3N\cdots{}^{\bullet}IO_3\cdots NH_3$	0.0230[b]/0.0529[c]	0.0517[b]/0.0706[c]	−0.0001[b]/−0.0128[c]

[a]All of the computed parameters are given in au. [b]The QTAIM topological parameters of R$^{\bullet}$ site-based interactions concerned with $H_3N\cdots{}^{\bullet}XO_3\cdots NH_3$. [c]The QTAIM topological parameters of R$^{\bullet}$-hole site-based interactions concerned with $H_3N\cdots{}^{\bullet}XO_3\cdots NH_3$.

At first glance, Figure 2 unveils the distributions of the electron density over and opposite to the surface of radical location, namely, R$^{\bullet}$ and R$^{\bullet}$-hole sites, respectively. Detailedly, an unconventional blue-colored R$^{\bullet}$ site was observed over the surface of the single electron of the studied molecules. The aforementioned observation outlined the potentiality of the studied halogens to act as Lewis acid centers via the R$^{\bullet}$ site and, accordingly, interact attractively with Lewis bases with disparate abilities (Figure 2). Notably, $V_{s,min}$ values were found to increase with enlargement of the atomic size of the halogens in the sequence $^{\bullet}ClO_3$ < $^{\bullet}BrO_3$ < $^{\bullet}IO_3$. Numerically, the positive EP magnitudes were 41.4, 51.2, and 52.2 kcal/mol for $^{\bullet}ClO_3$, $^{\bullet}BrO_3$, and $^{\bullet}IO_3$ molecules, respectively.

On the other hand, a positive R$^{\bullet}$-hole site was detected mirroring that of the single electron, disclosing the potency of the considered R$^{\bullet}$-bearing molecules to engage in R$^{\bullet}$-hole site-based interactions. This observation was in line with the literature that reported the R$^{\bullet}$-hole site was located at the centroid of the three coplanar atoms.[35] Regarding the R$^{\bullet}$-hole site, the $V_{s,max}$ calculations highlighted the anomalous order in the R$^{\bullet}$-hole size where it increased as follows: $^{\bullet}BrO_3$ < $^{\bullet}ClO_3$ < $^{\bullet}IO_3$. Overall, the forgoing manifestations would provide a proper corroboration for the potentiality of the inspected $^{\bullet}XO_3$ molecules to simultaneous engage in R$^{\bullet}$ and R$^{\bullet}$-hole site-based interactions.

Interaction Energy. To verify the efficacy of the investigated R$^{\bullet}$-bearing molecules to engage in R$^{\bullet}$ and R$^{\bullet}$-hole site-based interactions, the $NH_3\cdots{}^{\bullet}XO_3$ and $^{\bullet}XO_3\cdots NH_3$ dimers were constructed, respectively. Furthermore, the propensity of $^{\bullet}XO_3$ molecules to simultaneously interact via both sites was precisely examined within the $NH_3\cdots{}^{\bullet}XO_3\cdots NH_3$ trimers. Geometrical optimization was performed for all

https://doi.org/10.1021/acsomega.4c04620
ACS Omega 2024, 9, 38743−38752

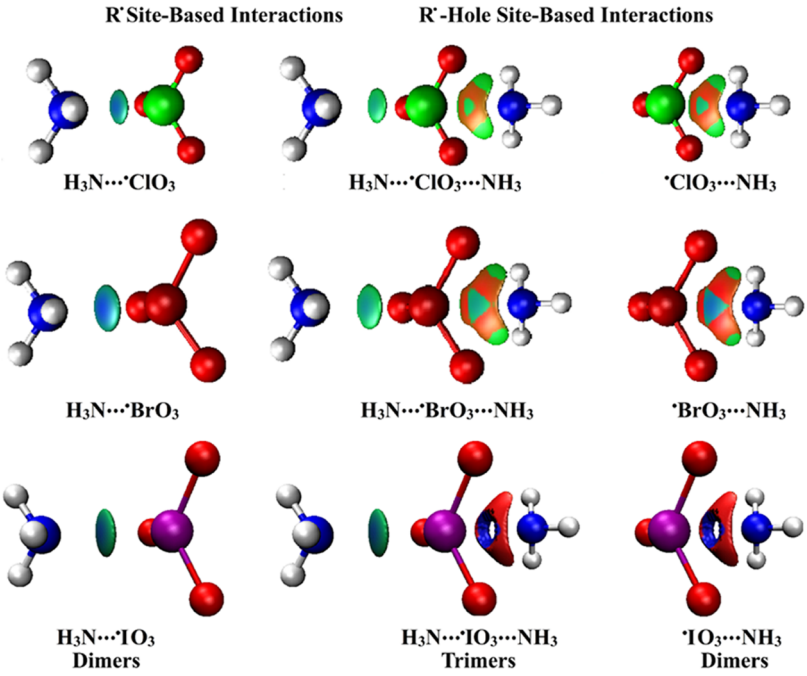

Figure 5. NCI isosurfaces of the dimeric and trimeric forms of R$^\bullet$ and R$^\bullet$-hole site-based interactions in the form of $NH_3\cdots{}^\bullet XO_3/{}^\bullet XO_3\cdots NH_3$ and $NH_3\cdots{}^\bullet XO_3\cdots NH_3$ complexes, respectively.

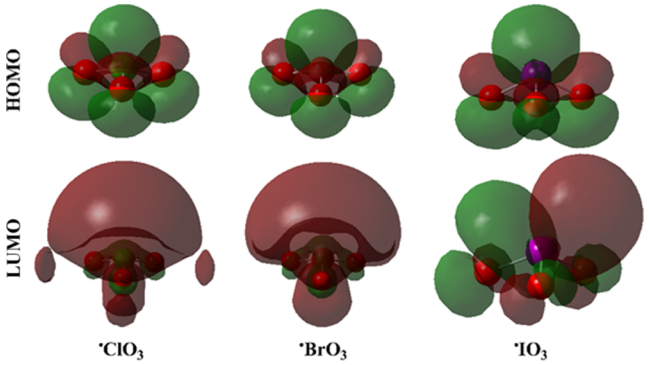

Figure 6. Plots of HOMO and LUMO distributions of the optimized $^\bullet ClO_3$, $^\bullet BrO_3$, and $^\bullet IO_3$ monomers.

of the studied complexes. The optimized geometries of the $NH_3\cdots{}^\bullet XO_3$, $^\bullet XO_3\cdots NH_3$, and $NH_3\cdots{}^\bullet XO_3\cdots NH_3$ complexes along with the optimum distances are displayed in Figure 3. Upon optimization of the complexes, interaction energies (E_{int}) were evaluated. Table 1 gathers the complexation parameters along with energetic features of all of the optimized $NH_3\cdots{}^\bullet XO_3/{}^\bullet XO_3\cdots NH_3$ dimers and $NH_3\cdots{}^\bullet XO_3\cdots NH_3$ trimers.

At first glance, all of the studied R$^\bullet$-bearing molecules demonstrated their apparent ability to engage in unconventional R$^\bullet$ site-based interactions and well-established R$^\bullet$-hole ones (Figure 3). Alongside, the optimum intermolecular distances were lower than the van der Waals (vdW) radii, ranging from 2.47 to 3.01 Å. Concerning $NH_3\cdots{}^\bullet XO_3$ dimers, negative E_{int} values were noted, asserting the impressive potentiality of the studied R$^\bullet$-bearing molecules to participate in R$^\bullet$ site-based interactions with a Lewis base. Obviously, the E_{int} was found to increase in line with growing positive EP size over the single-electron molecular surface (see Figure 2). For example, the E_{int} values were −6.01, −7.59, and −9.05 kcal/mol for the $NH_3\cdots{}^\bullet ClO_3$, $\cdots{}^\bullet BrO_3$, and $\cdots{}^\bullet IO_3$ dimers versus $V_{s,max}$ values of 41.4, 51.2, and 52.2 kcal/mol for the $^\bullet ClO_3$, $^\bullet BrO_3$, and $^\bullet IO_3$ molecules, respectively.

Turning to the R$^\bullet$-hole site-based interactions, a direct proportion was noticed between the atomic size of the studied group VII R$^\bullet$-bearing molecules and the E_{int} values of the $^\bullet XO_3\cdots NH_3$ dimers. This amplitude was in agreement with the previous findings of the tetrel-bearing molecules.[35] Illustratively, the E_{int} were found to increase as follows: $^\bullet ClO_3\cdots$ < $^\bullet BrO_3\cdots$ < $^\bullet IO_3\cdots NH_3$, amounting to −4.93, −6.44, and −14.82 kcal/mol, respectively. Such pattern reflected the imprecision perspective of $V_{s,max}$ affirmations relevant to the irregular correlation of the positive ESP with the R$^\bullet$ atomic size, as previously reported.[36]

Based upon the preceding observations, higher E_{int} values were perceived for the $NH_3\cdots{}^\bullet XO_3$ complexes over the $^\bullet XO_3\cdots NH_3$ ones when X = Cl and Br, highlighting the favorability of R$^\bullet$ site-based interactions over the R$^\bullet$-hole site-based ones. On the other hand, contradictory findings were obtained for iodine-bearing complexes.

Turning to the $NH_3\cdots{}^\bullet XO_3\cdots NH_3$ trimers, E_{int} was discerned to coincide with the energetic trends concerning the investigated dimers. Apparently, the E_{int} values were observed to follow the order: $NH_3\cdots{}^\bullet IO_3\cdots NH_3$ > $NH_3\cdots{}^\bullet BrO_3\cdots NH_3$ > $NH_3\cdots{}^\bullet ClO_3\cdots NH_3$ trimers with values of −19.89, −12.02, and −9.52 kcal/mol, respectively. Undoubtedly, impressive E_{int} values were registered for the $NH_3\cdots{}^\bullet XO_3\cdots NH_3$ trimers over those of the $NH_3\cdots{}^\bullet XO_3$ and $^\bullet XO_3\cdots NH_3$ dimers. For example, the E_{int} values of the $NH_3\cdots{}^\bullet IO_3$, $^\bullet IO_3\cdots NH_3$, and $NH_3\cdots{}^\bullet IO_3\cdots NH_3$ complexes were −9.05, −14.82, and −19.89 kcal/mol, respectively. The earlier observations evidently demonstrated the salient propensity of the considered R$^\bullet$-bearing molecules to simultaneously participate in R$^\bullet$ and R$^\bullet$-hole site-based interactions.

Moreover, the MP2 energetic features were benchmarked for the studied dimers and trimers by assessing E_{int} at the CCSD(T)/CBS level of theory. As listed in Table 1, the

https://doi.org/10.1021/acsomega.4c04620
ACS Omega 2024, 9, 38743−38752

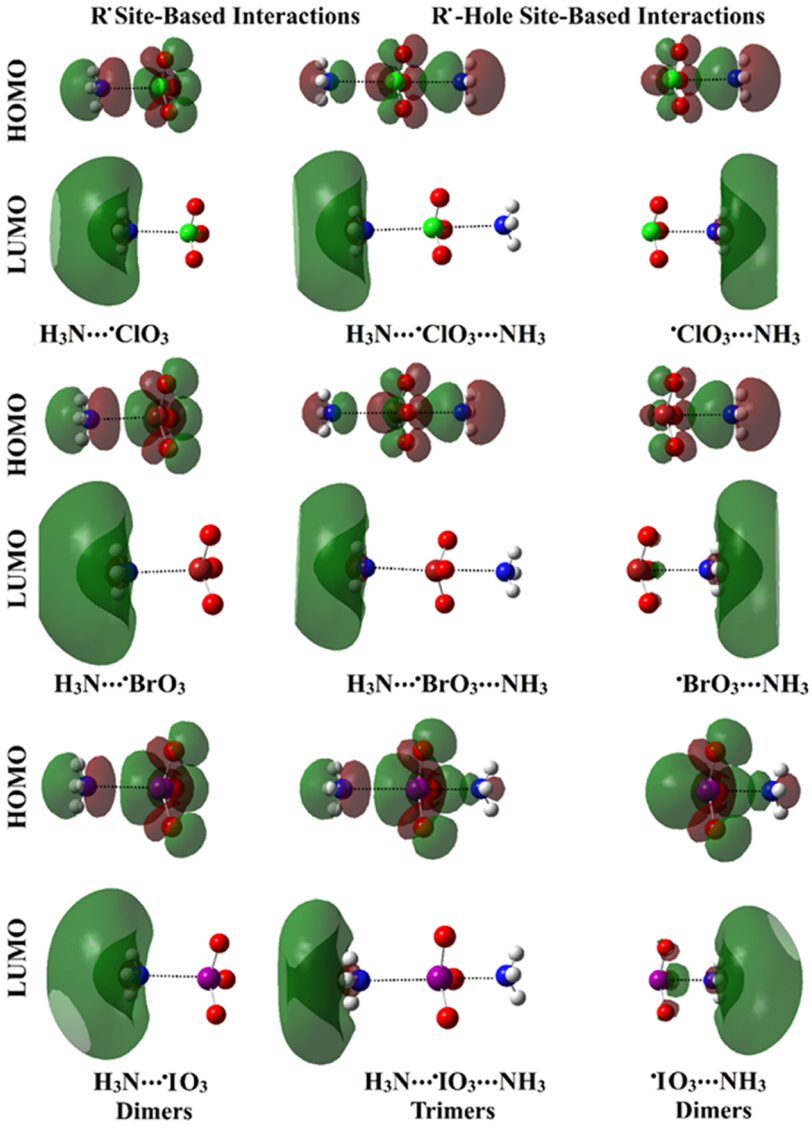

Figure 7. Plots of HOMO and LUMO distributions within the dimeric and trimeric forms of R$^\bullet$ and R$^\bullet$-hole site-based interactions in the form of $NH_3\cdots{}^\bullet XO_3/{}^\bullet XO_3\cdots NH_3$ and $NH_3\cdots{}^\bullet XO_3\cdots NH_3$ complexes, respectively.

CCSD(T)/CBS energetic results were found to be consistent with the MP2 ones. Numerically, the E_{int} values of the R$^\bullet$ site-based interactions were −5.90, −7.29, and −8.55 kcal/mol for the $NH_3\cdots{}^\bullet ClO_3$, $\cdots{}^\bullet BrO_3$, and $\cdots{}^\bullet IO_3$ dimers at the CCSD(T)/CBS level of theory along with E_{int} values of −6.01, −7.59, and −9.05 at the MP2 counterparts.

QTAIM Analysis. For a better understanding of the nature of the studied R$^\bullet$ and R$^\bullet$-hole site-based interactions, QTAIM[67] was employed. QTAIM diagrams of the $NH_3\cdots{}^\bullet XO_3$ and ${}^\bullet XO_3\cdots NH_3$ dimers, along with the $NH_3\cdots{}^\bullet XO_3\cdots NH_3$ trimers, are delineated in Figure 4. Topological parameters, including ρ_b, $\nabla^2\rho_b$, and H_b, are summarized in Table 2.

As delineated in Figure 4, solo BPs and BCPs were observed within all of the $NH_3\cdots{}^\bullet XO_3$ complexes, affirming the unconventional behavior exhibited by group VII elements toward efficiently engaging in the R$^\bullet$ site-based interactions with Lewis bases. The same remarks were obtained for the R$^\bullet$-hole site-based interactions that align with preceding studies.[36] Turning to the $NH_3\cdots{}^\bullet XO_3\cdots NH_3$ trimers, the potency of the R$^\bullet$-bearing molecules to simultaneously engage in R$^\bullet$ and R$^\bullet$-hole site-based interactions was emphasized via the presence of two BPs and BCPs (i.e., one at each site). These findings demonstrated the highly directional R$^\bullet$ and R$^\bullet$-hole site-based interactions of the investigated halogens.

As listed in Table 2, the closed-shell nature of the R$^\bullet$ and R$^\bullet$-hole site-based interactions was confirmed via the obtained positive values of $\nabla^2\rho_b$ and H_b along with the low values of ρ_b for the considered complexes, except for the iodine-bearing complexes. For the latter complexes, negative H_b values were detected, highlighting their partially covalent nature. Eminently, a notable correlation was found between the ρ_b values with the atomic size of the studied halogens and MP2 energetic values. Illustratively, the ρ_b of the R$^\bullet$ site-based interactions were 0.0236, 0.0255, and 0.0276 au of the $NH_3\cdots{}^\bullet ClO_3$, $\cdots{}^\bullet BrO_3$, and $\cdots{}^\bullet IO_3$ dimers, respectively, whose corresponding E_{int} values were −6.01, −7.59, and −9.05 kcal/mol.

NCI Analysis. The NCI index was earlier documented as a reliable tool to unveil the nature of the interactions between the chemical species three-dimensionally.[6] NCI isosurfaces were generated herein for the $NH_3\cdots{}^\bullet XO_3$ and ${}^\bullet XO_3\cdots NH_3$ dimers along with the $NH_3\cdots{}^\bullet XO_3\cdots NH_3$ trimers and are pictured in Figure 5. These isosurfaces are pictured through a

https://doi.org/10.1021/acsomega.4c04620
ACS Omega 2024, 9, 38743−38752

Table 3. E_{HOMO}, E_{LUMO}, E_{FL}, and E_{gap} of the R•-Bearing Molecules and Dimeric and Trimeric Forms of R• and R•-Hole Site-Based Interactions in the Form of $NH_3\cdots{}^{\bullet}XO_3/{}^{\bullet}XO_3\cdots NH_3$ and $NH_3\cdots{}^{\bullet}XO_3\cdots NH_3$ Complexes, Respectively, Given in eV

molecule/complex		E_{HOMO} (eV)	E_{LUMO} (eV)	E_{FL} (eV)	E_{gap} (eV)
monomers	R•-Bearing Molecules				
	$^{\bullet}ClO_3$	−14.26	−1.61	−7.94	12.65
	$^{\bullet}BrO_3$	−13.55	−2.18	−7.87	11.37
	$^{\bullet}IO_3$	−12.60	−0.67	−6.63	11.93
dimers	R• Site-Based Interactions				
	$H_3N\cdots{}^{\bullet}ClO_3$	−12.53	−0.73	−6.63	11.80
	$H_3N\cdots{}^{\bullet}BrO_3$	−12.74	−1.24	−6.99	11.50
	$H_3N\cdots{}^{\bullet}IO_3$	−12.46	−1.20	−6.83	11.26
	R•-Hole Site-Based Interactions				
	$^{\bullet}ClO_3\cdots NH_3$	−11.97	−0.90	−6.46	11.07
	$^{\bullet}BrO_3\cdots NH_3$	−12.12	−1.43	−6.78	10.69
	$^{\bullet}IO_3\cdots NH_3$	−0.12.27	−0.98	6.62	11.29
trimers	R• and R•-Hole Site-Based Interactions				
	$H_3N\cdots{}^{\bullet}ClO_3\cdots NH_3$	−11.58	−0.18	−5.88	11.40
	$H_3N\cdots{}^{\bullet}BrO_3\cdots NH_3$	−11.62	−0.71	−6.17	10.91
	$H_3N\cdots{}^{\bullet}IO_3\cdots NH_3$	−11.89	−0.10	−5.99	11.79

reduced density gradient (RDG) value of 0.50 au and colored from blue (sign $(\lambda_2)\rho$ = −0.035) to red (sign $(\lambda_2)\rho$ = 0.020).

As shown in Figure 5, the presence of the green-bluish-coded region between the interacting molecules evidently affirmed the occurrence of attractive forces within the complexes under study. Additionally, clear blue-coded regions were observed for the $NH_3\cdots{}^{\bullet}IO_3$, $^{\bullet}IO_3\cdots NH_3$, and $NH_3\cdots{}^{\bullet}IO_3\cdots NH_3$ complexes, highlighting their partially covalent nature, which was in line with the aforementioned QTAIM topological parameters. For almost all R•-hole hole site-based interactions, the contributions of the coplanar substituents to the total forces beyond the formation of the studied complexes were assured via the resulting shamrock shape, consistent with the previous studies.[36]

Electronic Parameters. To trace the electronic features, the FMO theory was asserted. In the FMO theory, the energy of the E_{HOMO}, E_{LUMO}, and E_{FL} were computed for the considered molecules and complexes. The E_{gap} was then assessed as the variation between the energies of the HOMO and LUMO. In the case of the singly occupied molecular orbital (SOMO), the distributions of the HOMO levels could be labeled as the SOMO patterns. The HOMO/LUMO electron densities were plotted for the isolated systems and complexes (Figures 6 and 7, respectively). E_{HOMO}, E_{LUMO}, E_{FL}, and E_{gap} values are tabulated in Table 3.

As shown in Figure 6, the HOMO and LUMO distributions of the investigated systems were noticed over the nucleophilic and electrophilic sites, respectively. After complexation, the distributions of HOMO and LUMO were drastically changed (Figure 7).

From Table 3, substantial changes in the E_{HOMO}, E_{LUMO}, E_{FL}, and E_{gap} values were prominently noted before and after interactions of the R•-bearing molecules with the Lewis base. For instance, the $E_{HOMO}/E_{LUMO}/E_{FL}/E_{gap}$ values of the $^{\bullet}ClO_3$ molecule were −14.26/−1.61/−7.94/12.65 eV that altered after complexation with NH_3 to −12.53/−0.73/−6.63/11.80 and −11.97/−0.90/−6.46/11.07 eV for $NH_3\cdots{}^{\bullet}ClO_3$ and $^{\bullet}ClO_3\cdots NH_3$ complexes, respectively.

A resurgent electron-donating character was noted for the investigated R•-bearing molecules on going from •Cl to •Br and •I, which was evidently reported via diminishing the E_{HOMO} values (i.e., less negative). For the inspected dimers, the higher preferability of R• site-based interactions over the R•-hole site-based ones was also affirmed via more positive E_{gap} for the $NH_3\cdots{}^{\bullet}XO_3$ complexes over the $^{\bullet}XO_3\cdots NH_3$ counterparts when X = Cl and Br. The reverse was confirmed for the iodine-bearing complexes, which was consistent with the energetic claims. Quantitatively, for the $NH_3\cdots{}^{\bullet}XO_3$ and $^{\bullet}XO_3\cdots NH_3$ dimers where X = Cl/Br/I, the E_{gap} were 11.80/11.50/11.26 and 11.07/10.69/11.29 accompanied by E_{int} of −6.01/−7.59/−9.05 and −4.93/−6.44/−14.82 kcal/mol, respectively. On the other hand, relatively less negative $E_{HOMO}/E_{LUMO}/E_{FL}$ and positive E_{gap} values were noted upon the formation of $H_3N\cdots{}^{\bullet}XO_3\cdots NH_3$ trimers compared to dimers. Such observations outlined the higher preferability of the trimeric form than that of the dimeric one for the studied systems.

Table 4. Global Indices of Reactivity of the R•-Bearing Molecules and Dimeric and Trimeric Forms of R• and R•-Hole Site-Based Interactions in the Form of $NH_3\cdots{}^{\bullet}XO_3/{}^{\bullet}XO_3\cdots NH_3$ and $NH_3\cdots{}^{\bullet}XO_3\cdots NH_3$ Complexes, Respectively

molecule/complex	system	IP (eV)	EA (eV)	μ (eV)	η (eV)	S (eV^{-1})	ω (eV)	Φ (eV)
monomers	R•-Bearing Molecules							
	$^{\bullet}ClO_3$	14.26	1.61	−7.94	6.32	0.16	4.98	7.94
	$^{\bullet}BrO_3$	13.55	2.18	−7.87	5.69	0.18	5.44	7.87
	$^{\bullet}IO_3$	12.60	0.67	−6.63	5.97	0.17	3.68	6.63
dimers	R• Site-Based Interactions							
	$H_3N\cdots{}^{\bullet}ClO_3$	12.53	0.73	−6.63	5.90	0.17	3.72	6.63
	$H_3N\cdots{}^{\bullet}BrO_3$	12.74	1.24	−6.99	5.75	0.17	4.25	6.99
	$H_3N\cdots{}^{\bullet}IO_3$	12.46	1.20	−6.83	5.63	0.18	4.14	6.83
	R•-Hole Site-Based Interactions							
	$^{\bullet}ClO_3\cdots NH_3$	11.97	0.90	−6.43	5.54	0.18	3.74	6.43
	$^{\bullet}BrO_3\cdots NH_3$	12.12	1.43	−6.78	5.34	0.19	4.30	6.78
	$^{\bullet}IO_3\cdots NH_3$	12.27	0.98	−6.62	5.65	0.18	3.88	6.62
trimers	R• and R•-Hole Site-Based Interactions							
	$H_3N\cdots{}^{\bullet}ClO_3\cdots NH_3$	11.58	0.18	−5.88	5.70	0.18	3.03	5.88
	$H_3N\cdots{}^{\bullet}BrO_3\cdots NH_3$	11.62	0.71	−6.17	5.45	0.18	3.49	6.17
	$H_3N\cdots{}^{\bullet}IO_3\cdots NH_3$	11.89	0.10	−5.99	5.89	0.17	3.05	5.99

https://doi.org/10.1021/acsomega.4c04620
ACS Omega 2024, 9, 38743−38752

Global Indices of Reactivity. In an effort to unveil the chemical reactivity of the radical species to participate in several noncovalent interactions, global indices of reactivity were assessed before and after the occurrence of the studied interactions. Various global reactivity indices, including EA, S, η, IP, ω, μ, and Φ, were assessed (Table 4).

Upon the complexation of the investigated R$^\bullet$-bearing molecules with the NH_3 Lewis base via the R$^\bullet$ and R$^\bullet$-hole sites, drastic differences in the reactivity parameters were noted in the form of studied dimers and trimers (Table 4). Numerically, the $^\bullet IO_3$ molecule had IP/EA/μ/η/S/ω/Φ values of 12.60/0.67/−6.63/5.97/0.17/3.68/6.63 eV that changed to 12.46/1.20/−6.83/5.63/0.18/4.14/6.83, 12.27/0.98/−6.62/5.65/0.18/3.88/6.62, and 11.89/0.10/−5.99/5.89/0.17/3.05/5.99 eV in the case of the $H_3N\cdots{}^\bullet IO_3$, $^\bullet IO_3\cdots H_3N$, and $H_3N\cdots{}^\bullet IO_3\cdots H_3N$ complexes, respectively. These findings assured the alteration of electronic parameters before and after the complexation, outlining the occurrence of the investigated interactions.

CONCLUSIONS

The predilection of R$^\bullet$-bearing molecules to engage in the unconventional R$^\bullet$ site-based interactions and the well-established R$^\bullet$-hole site-based interactions was comparatively studied. Accordingly, various MP2 computations were performed and analyzed for the $NH_3\cdots{}^\bullet XO_3$, $^\bullet XO_3\cdots NH_3$ and $NH_3\cdots{}^\bullet XO_3\cdots NH_3$ complexes. EP analyses enunciated the presence of positive blue-coded regions over and opposite the molecular surface of the single electron, namely, R$^\bullet$ and R$^\bullet$-hole sites, respectively. MP2 energies also accentuated the noteworthy potentiality of the studied molecules to engage in R$^\bullet$ and R$^\bullet$-hole site-based interactions with a higher preferability for the former interactions in the case of chlorine- and bromine-bearing complexes. The latter trend was reversed in the case of the iodine-bearing complexes. A direct correlation was also disclosed between the E_{int} values and the atomic sizes of the studied halogen (X) atoms. QTAIM and NCI affirmations outlined the closed-shell nature of the R$^\bullet$ and R$^\bullet$-hole site-based interactions except for the iodine-bearing complexes that were detected with a partially covalent one. Overall, these results will support the forthcoming studies for the characterization and applications of R$^\bullet$ and R$^\bullet$-hole site-based interactions.

ASSOCIATED CONTENT

Supporting Information

The Supporting Information is available free of charge at https://pubs.acs.org/doi/10.1021/acsomega.4c04620.

Cartesian atomic coordinates and expectation value of the S_2 operator value of the optimized $NH_3\cdots{}^\bullet XO_3/{}^\bullet XO_3\cdots NH_3$ and $NH_3\cdots{}^\bullet XO_3\cdots NH_3$ complexes (where X = Cl, Br, and I) (PDF)

AUTHOR INFORMATION

Corresponding Authors

Mahmoud A. A. Ibrahim − *Computational Chemistry Laboratory, Chemistry Department, Faculty of Science, Minia University, Minia 61519, Egypt; School of Health Sciences, University of KwaZulu-Natal, Durban 4000, South Africa;* orcid.org/0000-0003-4819-2040; Email: m.ibrahim@compchem.net

Tamer Shoeib − *Department of Chemistry, The American University in Cairo, New Cairo 11835, Egypt;* orcid.org/0000-0003-3512-1593; Email: t.shoeib@aucegypt.edu

Authors

Heba S. M. Abd Elhafez − *Computational Chemistry Laboratory, Chemistry Department, Faculty of Science, Minia University, Minia 61519, Egypt*

Mohammed N. I. Shehata − *Computational Chemistry Laboratory, Chemistry Department, Faculty of Science, Minia University, Minia 61519, Egypt;* orcid.org/0000-0002-3334-6070

Nayra A. M. Moussa − *Computational Chemistry Laboratory, Chemistry Department, Faculty of Science, Minia University, Minia 61519, Egypt; Basic and Clinical Medical Science Department, Faculty of Dentistry, Deraya University, New Minya 61768, Egypt;* orcid.org/0000-0003-3712-7710

Shaban R. M. Sayed − *Department of Botany and Microbiology, College of Science, King Saud University, Riyadh 11451, Saudi Arabia*

Mahmoud E. S. Soliman − *Molecular Bio-Computation and Drug Design Research Laboratory, School of Health Sciences, University of KwaZulu-Natal, Durban 4000, South Africa;* orcid.org/0000-0002-8711-7783

Muhammad Naeem Ahmed − *Department of Chemistry, The University of Azad Jammu and Kashmir, Muzaffarabad 13100, Pakistan*

Mohamed Khaled Abd El-Rahman − *Department of Chemistry and Chemical Biology, Harvard University, Cambridge, Massachusetts 02138, United States*

Complete contact information is available at: https://pubs.acs.org/10.1021/acsomega.4c04620

Author Contributions

M.A.A.I.: Conceptualization, methodology, software, resources, project administration, supervision, writing—review and editing. H.S.M.A.E.: Data curation, formal analysis, investigation, visualization, writing—original draft. M.N.I.S.: Methodology, investigation, project administration, writing—review and editing. N.A.M.M.: Methodology, investigation, project administration, writing—review and editing. S.R.M.S.: Resources, writing—review and editing. M.E.S.S.: Resources, writing—review and editing. M.N.A.: Visualization, writing—review and editing. M.K.A.E.-R.: Writing—review and editing. T.S.: Conceptualization, resources, methodology, writing—review and editing.

Notes

The authors declare no competing financial interest.

ACKNOWLEDGMENTS

The authors extend their appreciation to the Researchers Supporting Project number (RSPD2024R743), King Saud University, Riyadh, Saudi Arabia, for funding this work. The computational work was completed with resources provided by the CompChem Lab (Minia University, Egypt, hpc.compchem.net), Center for High-Performance Computing (Cape Town, South Africa, http://www.chpc.ac.za), Bibliotheca Alexandrina (http://hpc.bibalex.org), and the American University in Cairo.

REFERENCES

(1) Mahmudov, K. T.; Gurbanov, A. V.; Guseinov, F. I.; da Silva, M. F. C. G. Noncovalent interactions in metal complex catalysis. *Coord. Chem. Rev.* **2019**, *387*, 32−46.

(2) Jiang, S.; Zhang, L.; Cui, D.; Yao, Z.; Gao, B.; Lin, J.; Wei, D. The Important Role of Halogen Bond in Substrate Selectivity of Enzymatic Catalysis. *Sci. Rep.* **2016**, *6*, No. 34750.

(3) Lu, Y.; Liu, Y.; Xu, Z.; Li, H.; Liu, H.; Zhu, W. Halogen bonding for rational drug design and new drug discovery. *Expert Opin. Drug Discovery* **2012**, *7*, 375−383.

(4) Lu, Y.; Wang, Y.; Zhu, W. Nonbonding interactions of organic halogens in biological systems: Implications for drug discovery and biomolecular design. *Phys. Chem. Chem. Phys.* **2010**, *12*, 4543−4551.

(5) Mendez, L.; Henriquez, G.; Sirimulla, S.; Narayan, M. Looking back, looking forward at halogen bonding in drug discovery. *Molecules* **2017**, *22*, 1397.

(6) Johnson, E. R.; Keinan, S.; Mori-Sanchez, P.; Contreras-Garcia, J.; Cohen, A. J.; Yang, W. Revealing noncovalent interactions. *J. Am. Chem. Soc.* **2010**, *132*, 6498−6506.

(7) Huang, Z.; Qin, K.; Deng, G.; Wu, G.; Bai, Y.; Xu, J. F.; Wang, Z.; Yu, Z.; Scherman, O. A.; Zhang, X. Supramolecular chemistry of cucurbiturils: Tuning cooperativity with multiple noncovalent interactions from positive to negative. *Langmuir* **2016**, *32*, 12352−12360.

(8) Bartkowski, M.; Giordani, S. Supramolecular chemistry of carbon nano-onions. *Nanoscale* **2020**, *12*, 9352−9358.

(9) Li, Z.-T.; Wu, L.-Z. *Hydrogen Bonded Supramolecular Structures*; Springer, 2015; Vol. *87*.

(10) Davis, A. P.; Wareham, R. S. Carbohydrate recognition through noncovalent interactions: A challenge for biomimetic and supramolecular chemistry. *Angew. Chem., Int. Ed.* **1999**, *38*, 2978−2996.

(11) Mazik, M. Molecular recognition of carbohydrates by acyclic receptors employing noncovalent interactions. *Chem. Soc. Rev.* **2009**, *38*, 935−956.

(12) Schalley, C. A. Supramolecular chemistry goes gas phase: the mass spectrometric examination of noncovalent interactions in host−guest chemistry and molecular recognition. *Int. J. Mass Spectrom.* **2000**, *194*, 11−39.

(13) Fish, R. H.; Jaouen, G. Bioorganometallic chemistry: Structural diversity of organometallic complexes with bioligands and molecular recognition studies of several supramolecular hosts with biomolecules, alkali-metal ions, and organometallic pharmaceuticals. *Organometallics* **2003**, *22*, 2166−2177.

(14) Mó, O. Some interesting features of the rich chemistry around electron-deficient systems. *Pure Appl. Chem.* **2020**, *92*, 773−787.

(15) Politzer, P.; Lane, P.; Concha, M. C.; Ma, Y.; Murray, J. S. An overview of halogen bonding. *J. Mol. Model.* **2007**, *13*, 305−311.

(16) Clark, T.; Hennemann, M.; Murray, J. S.; Politzer, P. Halogen bonding: the sigma-hole. *J. Mol. Model.* **2007**, *13*, 291−296.

(17) Angarov, V.; Kozuch, S. On the σ, π and δ hole interactions: A molecular orbital overview. *New J. Chem.* **2018**, *42*, 1413−1422.

(18) Varadwaj, P. R.; Varadwaj, A.; Marques, H.; Yamashita, K. Can combined electrostatic and polarization effects alone explain the F···F negative-negative bonding in simple fluoro-substituted benzene derivatives? A first-principles perspective. *Computation* **2018**, *6*, 51−84.

(19) Brammer, L. Halogen bonding, chalcogen bonding, pnictogen bonding, tetrel bonding: origins, current status and discussion. *Faraday Discuss.* **2017**, *203*, 485−507.

(20) Varadwaj, A.; Marques, H. M.; Varadwaj, P. R. Is the fluorine in molecules dispersive? Is molecular electrostatic potential a valid property to explore fluorine-centered non-covalent interactions? *Molecules* **2019**, *24*, 379−407.

(21) Alkorta, I.; Elguero, J.; Frontera, A. Not only hydrogen bonds: Other noncovalent interactions. *Crystals* **2020**, *10*, 180−208.

(22) Politzer, P.; Murray, J. S.; Clark, T.; Resnati, G. The sigma-hole revisited. *Phys. Chem. Chem. Phys.* **2017**, *19*, 32166−32178.

(23) Ibrahim, M. A. A.; Saeed, R. R. A.; Shehata, M. N. I.; Ahmed, M. N.; Shawky, A. M.; Khowdiary, M. M.; Elkaeed, E. B.; Soliman, M. E. S.; Moussa, N. A. M. Type I−IV halogen···halogen interactions: A comparative theoretical study in halobenzene···halobenzene homodimers. *Int. J. Mol. Sci.* **2022**, *23*, 3114.

(24) Ibrahim, M. A. A.; Shehata, M. N. I.; Rady, A. S. M.; Abuelliel, H. A. A.; Abd Elhafez, H. S. M.; Shawky, A. M.; Oraby, H. F.; Hasanin, T. H. A.; Soliman, M. E. S.; Moussa, N. A. M. Effects of Lewis basicity and acidity on sigma-hole interactions in carbon-bearing complexes: A comparative ab initio study. *Int. J. Mol. Sci.* **2022**, *23*, 13023.

(25) Ibrahim, M. A. A.; Shehata, M. N. I.; Soliman, M. E. S.; Moustafa, M. F.; El-Mageed, H. R. A.; Moussa, N. A. M. Unusual chalcogen···chalcogen interactions in like···like and unlike Y = C=Y··· Y = C=Y complexes (Y = O, S, and Se). *Phys. Chem. Chem. Phys.* **2022**, *24*, 3386−3399.

(26) Murray, J. S.; Politzer, P. The electrostatic potential: An overview. *Wiley Interdiscip. Rev.: Comput. Mol. Sci.* **2011**, *1*, 153−163.

(27) Frontera, A. σ- and π-Hole Interactions. *Crystals* **2020**, *10*, 721.

(28) Ibrahim, M. A. A.; Saeed, R. R. A.; Shehata, M. N. I.; Mohamed, E. E. B.; Soliman, M. E. S.; Al-Fahemi, J. H.; El-Mageed, H. R. A.; Ahmed, M. N.; Shawky, A. M.; Moussa, N. A. M. Unexplored σ-hole and π-hole interactions in (X2CY)2 complexes (X = F, Cl; Y = O, S). *J. Mol. Struct.* **2022**, *1265*, No. 133232.

(29) Politzer, P.; Murray, J. S.; Clark, T. The pi-hole revisited. *Phys. Chem. Chem. Phys.* **2021**, *23*, 16458−16468.

(30) Bauza, A.; Frontera, A.; Mooibroek, T. J. pi-Hole interactions involving nitro aromatic ligands in protein structures. *Chemistry* **2019**, *25*, 13436−13443.

(31) Ibrahim, M. A. A.; Saeed, R. R. A.; Shehata, M. N. I.; Moussa, N. A. M.; Tawfeek, A. M.; Ahmed, M. N.; Abd El-Rahman, M. K.; Shoeib, T. Sigma-hole and lone-pair-hole site-based interactions of seesaw tetravalent chalcogen-bearing molecules with Lewis bases. *ACS Omega* **2023**, *8*, 32828−32837.

(32) Bauza, A.; Mooibroek, T. J.; Frontera, A. Sigma-hole opposite to a lone pair: Unconventional pnicogen bonding interactions between ZF3 (Z = N, P, As, and Sb) compounds and several donors. *ChemPhysChem* **2016**, *17*, 1608−1614.

(33) Shukla, R.; Yu, D.; Mu, T.; Kozuch, S. Yet another perspective on hole interactions, part II: lp-hole *vs.* lp-hole interactions. *Phys. Chem. Chem. Phys.* **2023**, *25*, 12641−12649.

(34) Del Bene, J. E.; Alkorta, I.; Elguero, J.; Sanchez-Sanz, G. Lone-pair hole on P: P···N pnicogen bonds assisted by halogen bonds. *J. Phys. Chem. A* **2017**, *121*, 1362−1370.

(35) Ibrahim, M. A. A.; Telb, E. M. Z. Comparison of ± σ-hole and ± R-hole interactions formed by tetrel-containing complexes: a computational study. *RSC Adv.* **2021**, *11*, 4011−4021.

(36) Ibrahim, M. A. A.; Mohamed, Y. A. M.; Abd Elhafez, H. S. M.; Shehata, M. N. I.; Soliman, M. E. S.; Ahmed, M. N.; Abd El-Mageed, H. R.; Moussa, N. A. M. R●-hole interactions of group IV-VII radical-containing molecules: A comparative study. *J. Mol. Graph. Model.* **2022**, *111*, No. 108097.

(37) Wang, Y.-H.; Zou, J.-W.; Lu, Y.-X.; Yu, Q.-S.; Xu, H.-Y. Single-electron halogen bond: Ab initio study. *Int. J. Quantum Chem.* **2007**, *107*, 501−506.

(38) Alkorta, I.; Elguero, J.; Solimannejad, M. Single electron pnicogen bonded complexes. *J. Phys. Chem. A* **2014**, *118*, 947−953.

(39) Li, Y.; Wu, D.; Li, Z. R.; Chen, W.; Sun, C. C. Do single-electron lithium bonds exist? Prediction and characterization of the H3C···Li-Y (Y = H, F, OH, CN, NC, and CCH) complexes. *J. Chem. Phys.* **2006**, *125*, No. 084317.

(40) Li, Z. F.; Yang, X. P.; DeYonker, N. J.; Xu, X. Y.; Guo, Z.; Zhao, C. Y. Binding energies and interaction origins between nonclassical single-electron hydrogen, sodium and lithium bonds and neutral boron-containing radicals: a theoretical investigation. *China Sci. Bull.* **2014**, *59*, 2597−2607.

(41) Yu, D.; Wu, D.; Li, Y.; Li, S. Y. On the formation of beryllium bonds where radicals act as electron donors. *Theor. Chem. Acc.* **2016**, *135*, 112.

(42) Merritt, J. M.; Rudic, S.; Miller, R. E. Infrared laser spectroscopy of CH3···HF in helium nanodroplets: The exit-channel

https://doi.org/10.1021/acsomega.4c04620
ACS Omega 2024, 9, 38743−38752

complex of the F + CH4 reaction. *J. Chem. Phys.* **2006**, *124*, No. 084301.
(43) Tachikawa, H. A direct ab initio dynamics study on the finite temperature effects on the hyperfine coupling constant of a weakly bonded complex. *J. Phys. Chem. A* **1998**, *102*, 7065−7069.
(44) Misochko, E. Y.; Benderskii, V. A.; Goldschleger, A. U.; Akimov, A. V.; Shestakov, A. F. Formation of the CH3-HF complex in reaction of thermal F atoms with CH4 in solid Ar. *J. Am. Chem. Soc.* **1995**, *117*, 11997−11998.
(45) Alkorta, I.; Rozas, I.; Elguero, J. Radicals as hydrogen bond acceptors. *Ber. Bunsen-Ges. Phys. Chem.* **1998**, *102*, 429−435.
(46) An, X.; Liu, H.; Li, Q.; Gong, B.; Cheng, J. Influence of substitution, hybridization, and solvent on the properties of C-HO single-electron hydrogen bond in CH_3-H_2O complex. *J. Phys. Chem. A* **2008**, *112*, 5258−5263.
(47) Hammerum, S. Alkyl radicals as hydrogen bond acceptors: computational evidence. *J. Am. Chem. Soc.* **2009**, *131*, 8627−8635.
(48) Rudić, S.; Merritt, J. M.; Miller, R. E. Study of the CH3 H2O radical complex stabilized in helium nanodroplets. *Phys. Chem. Chem. Phys.* **2009**, *11*, 5345−5352.
(49) Li, Q.; An, X.; Luan, F.; Li, W.; Gong, B.; Cheng, J.; Sun, J. Cooperativity between two types of hydrogen bond in H(3)C-HCN-HCN and H(3)C-HNC-HNC complexes. *J. Chem. Phys.* **2008**, *128*, No. 154102.
(50) Rudić, S.; Merritt, J. M.; Miller, R. E. Infrared laser spectroscopy of the CH_3-HCN radical complex stabilized in helium nanodroplets. *J. Chem. Phys.* **2006**, *124*, No. 104305.
(51) Solimannejad, M.; Alikhani, M. E. Theoretical study of the HCN-CH and HNC-CH radicals: Hydrogen and covalent bonding. *Chem. Phys. Lett.* **2005**, *406*, 351−354.
(52) Wang, B.-Q.; Li, Z.-R.; Wu, D.; Hao, X.-Y.; Li, R.-J.; Sun, C.-C. Single-electron hydrogen bonds in the methyl radical complexes H3C···HF and H3C···HCCH: an ab initio study. *Chem. Phys. Lett.* **2003**, *375*, 91−95.
(53) Frisch, J.; Trucks, G. W.; Schlegel, H. B.; Scuseria, G. E.; Robb, M. A.; Cheeseman, J. R.; Scalmani, G.; Barone, V.; Mennucci, B.; Petersson, G. A.; Nakatsuji, H.; Caricato, M.; Li, X.; Hratchian, H. P.; Izmaylov, A. F.; Bloino, J.; Zheng, G.; Sonnenberg, J. L.; Hada, M.; Ehara, M.; Toyota, K.; Fukuda, R.; Hasegawa, J.; Ishida, M.; Nakajima, T.; Honda, Y.; Kitao, O.; Nakai, H.; Vreven, T.; Montgomery, J. A., Jr.; Peralta, J. E.; Ogliaro, F.; Bearpark, M.; Heyd, J. J.; Brothers, E.; Kudin, K. N.; Staroverov, V. N.; Kobayashi, R.; Normand, J.; Raghavachari, K.; Rendell, A.; Burant, J. C.; Iyengar, S. S.; Tomasi, J.; Cossi, M.; Rega, N.; Millam, J. M.; Klene, M.; Knox, J. E.; Cross, J. B.; Bakken, V.; Adamo, C.; Jaramillo, J.; Gomperts, R.; Stratmann, R. E.; Yazyev, O.; Austin, A. J.; Cammi, R.; Pomelli, C.; Ochterski, J. W.; Martin, R. L.; Morokuma, K.; Zakrzewski, V. G.; Voth, G. A.; Salvador, P.; Dannenberg, J. J.; Dapprich, S.; Daniels, A. D.; Farkas, Ö.; Foresman, J. B.; Ortiz, J. V.; Cioslowski, J.; Fox, D. J.; et al. *Gaussian 09*, revision E.01; Gaussian, Inc.: Wallingford CT, 2009.
(54) Møller, C.; Plesset, M. S. Note on an approximation treatment for many-electron systems. *Phys. Rev.* **1934**, *46*, 618−622.
(55) Kendall, R. A.; Dunning, T. H.; Harrison, R. J. Electron affinities of the first-row atoms revisited. Systematic basis sets and wave functions. *J. Chem. Phys.* **1992**, *96*, 6796−6806.
(56) Woon, D. E.; Dunning, T. H. Gaussian basis sets for use in correlated molecular calculations. III. The atoms aluminum through argon. *J. Chem. Phys.* **1993**, *98*, 1358−1371.
(57) Peterson, K. A.; Figgen, D.; Goll, E.; Stoll, H.; Dolg, M. Systematically convergent basis sets with relativistic pseudopotentials. II. Small-core pseudopotentials and correlation consistent basis sets for the post-d group 16−18 elements. *J. Chem. Phys.* **2003**, *119*, 11113−11123.
(58) Peterson, K. A.; Shepler, B. C.; Figgen, D.; Stoll, H. On the Spectroscopic and Thermochemical Properties of ClO, BrO, IO, and Their Anions. *J. Phys. Chem. A* **2006**, *110*, 13877−13883.
(59) Pritchard, B. P.; Altarawy, D.; Didier, B.; Gibson, T. D.; Windus, T. L. New basis set exchange: An open, up-to-date resource for the molecular sciences community. *J. Chem. Inf. Model.* **2019**, *59*, 4814−4820.
(60) Feller, D. The role of databases in support of computational chemistry calculations. *J. Comput. Chem.* **1996**, *17*, 1571−1586.
(61) Schuchardt, K. L.; Didier, B. T.; Elsethagen, T.; Sun, L.; Gurumoorthi, V.; Chase, J.; Li, J.; Windus, T. L. Basis set exchange: A community database for computational sciences. *J. Chem. Inf. Model.* **2007**, *47*, 1045−1052.
(62) Ibrahim, M. A. A. Molecular mechanical perspective on halogen bonding. *J. Mol. Model.* **2012**, *18*, 4625−4638.
(63) Lu, T.; Chen, F. Multiwfn: a multifunctional wavefunction analyzer. *J. Comput. Chem.* **2012**, *33*, 580−592.
(64) Boys, S. F.; Bernardi, F. The calculation of small molecular interactions by the differences of separate total energies. Some procedures with reduced errors. *Mol. Phys.* **1970**, *19*, 553−566.
(65) Mishra, B. K.; Karthikeyan, S.; Ramanathan, V. Tuning the C-H···Pi interaction by different substitutions in benzene-acetylene complexes. *J. Chem. Theory Comput.* **2012**, *8*, 1935−1942.
(66) Helgaker, T.; Klopper, W.; Koch, H.; Noga, J. Basis-set convergence of correlated calculations on water. *J. Chem. Phys.* **1997**, *106*, 9639−9646.
(67) Bader, R. F. W. Atoms in molecules. *Acc. Chem. Res.* **1985**, *18*, 9−15.
(68) Humphrey, W.; Dalke, A.; Schulten, K. VMD: Visual molecular dynamics. *J. Mol. Graph.* **1996**, *14*, 33−38.
(69) Weiner, P. K.; Langridge, R.; Blaney, J. M.; Schaefer, R.; Kollman, P. A. Electrostatic potential molecular surfaces. *Proc. Natl. Acad. Sci. U.S.A.* **1982**, *79*, 3754−3758.

https://doi.org/10.1021/acsomega.4c04620
ACS Omega 2024, 9, 38743−38752